PROCEEDINGS OF SCIENCE

Strong Multiple Higgs Production at CLIC

Andrea Thamm*
CERN, Physics Department, Theory Division, CH-1211 Geneva 23, Switzerland
Institut de Théorie des Phénomènes Physiques, EPFL, CH-1015 Lausanne, Switzerland
E-mail: andrea.thamm@cern.ch

To make precision measurements on a Higgs-like scalar particle, a multi-TeV linear electron-positron collider such as the future Compact Linear Collider (CLIC) would set the ideal environment. We present results on the CLIC reach on the parameter space of the minimal composite Higgs model which describes a light composite Higgs emerging as a pseudo-Nambu Goldstone (NG) boson in the breaking of a strongly coupled sector. The specific feature of this model is the energy growth of NG boson scattering amplitudes, i.e. the longitudinally polarized vector bosons and the Higgs. We study double Higgs production in electron positron collisions and obtain an estimate of the CLIC sensitivity on the anomalous Higgs couplings. In order to estimate its sensitivity on the compositeness scale, double Higgs production proves to be the most important process which can probe scales up to 30 TeV. Moreover, we find that the study of triple Higgs production can provide deeper insight into the underlying structure of the coset space and enable us to distinguish between a symmetric and asymmetric coset space or a non-sigma model.

Proceedings of the Corfu Summer Institute 2011 School and Workshops on Elementary Particle Physics and Gravity
September 4-18, 2011
Corfu, Greece

*Speaker.

PoS(CORFU2011)035

1. Motivation and Results

Within the last year, the search for the long predicted elementary scalar particle, the Higgs boson, got more and more conclusive. The most recent analyses of data from all experiments, both ATLAS [1] and CMS [2] at the LHC as well as CDF and D0 at the Tevatron [3], are pointing towards the existence of a relatively light SM-like Higgs boson with a mass around $m_h \sim 125$ GeV [4]. The current 8 TeV run at the LHC will most likely give a definite answer about discovery or exclusion of the SM Higgs boson by the end of this year.

Provided a light Higgs-like scalar, h, will be found, its properties need to be studied carefully in order to establish a clear description of the dynamics of electroweak symmetry breaking and to distinguish between various possible models. As a proton-proton collider, the LHC will probably not be able to deliver the precision required to explore the parameter space of models with only heavy new states [5, 6]. In such a situation, a linear electron-positron collider would be the machine of choice since, due to its clean collision environment, it could consolidate the results of the LHC and, moreover, make precision measurements [7]. CLIC [8] and the International Linear Collider (ILC) [9] are two independent projects designing a future linear collider. While the ILC has a design centre of mass energy of $\sqrt{s} = 500$ GeV, CLIC is a multi-TeV linear collider with a design centre of mass energy of $\sqrt{s} = 3$ TeV with a potential upgrade to $\sqrt{s} = 5$ TeV.

We have studied the physics reach of such a linear collider on a new strongly coupled sector at the TeV-scale. This new sector is assumed to obey a global symmetry which is spontaneously broken down to a subgroup at the scale f. One example is the the minimal composite Higgs model $SO(5)/SO(4)$ [10 – 14]. In addition to the three NG bosons which are eaten by the SM gauge bosons to make them massive, in this example also a Higgs-like scalar emerges in the breaking as the fourth NG boson. Although the Higgs boson can be very SM like in the limit of a very large compositeness scale, it is now a bound state of new strongly interacting particles and will therefore have modified couplings to the gauge bosons and to itself with respect to a SM Higgs. A general parameterization of these deviations looks as follows [6]:

$$\begin{aligned}\mathscr{L} =& \frac{1}{2}\left(\partial_\mu h\right)^2 - V(h) + \frac{v^2}{2}\left(D_\mu \Sigma^\dagger D^\mu \Sigma\right)\left[1 + 2a\frac{h}{v} + b\frac{h^2}{v^2} + b_3\frac{h^3}{v^3}\ldots\right] + \ldots \\ &+ m_i \bar{\psi}_{Li}\Sigma\left(1 + c\frac{h}{v}\ldots\right)\psi_{Ri} + h.c.\end{aligned} \tag{1.1}$$

where $v = 246$ GeV, the three NG bosons π^a are described by $\Sigma = \exp^{\frac{i}{v}\sigma_a\pi^a}$, with σ_a denoting the Pauli matrices, and the Higgs potential $V(h)$ is of the form:

$$V(h) = \frac{1}{2}m_h^2 h^2 + d_3\left(\frac{m_h^2}{2v}\right)h^3 + d_4\left(\frac{m_h^2}{8v^2}\right)h^4 + \ldots . \tag{1.2}$$

The parameters a, b, b_3 and d_4 can be expressed in terms of $\xi = \frac{v^2}{f^2}$ which characterizes the model and measures the scale of compositeness, i.e. the typical mass scale of the heavy resonances $m_\rho = g_\rho f$, where g_ρ is the strong coupling. For instance, in the minimal $SO(5)/SO(4)$ composite Higgs model the relations are:

$$
\begin{array}{lll}
a=\sqrt{1-\xi}, & b=1-2\xi, & b_3=-\frac{4}{3}\xi\sqrt{1-\xi} \\
d_3=c=\sqrt{1-\xi} & d_4=1-\frac{7}{3}\xi & \text{spinorial representation of SO(5)} \\
d_3=c=\frac{1-2\xi}{\sqrt{1-\xi}} & d_4=\frac{1-28\xi(1-\xi)/3}{1-\xi} & \text{fundamental representation of SO(5)}
\end{array}
\tag{1.3}
$$

While a controls the strength of longitudinal gauge boson scattering $V_LV_L \to V_LV_L$, and b is related to double Higgs production $V_LV_L \to hh$, b_3 is sensitive to triple Higgs production $V_LV_L \to hhh$. The cross sections of some of these processes are growing with the energy which is the crucial feature that distinguishes a NG boson Higgs from the SM one. The SM corresponds to $\xi = 0$ and therefore $a = b = c = d_3 = d_4 = 1$ and $b_3 = 0$ and all the higher order terms vanishing.

The sensitivity of the LHC on the model-specific parameters was studied in Ref. [6]. Vector boson scattering is feasible at the LHC thanks to the relatively clean final state in the partonic channel $W_LW_L \to \ell\ell + \not{E}_T$. At 14 TeV and 300 fb^{-1} integrated luminosity this process is accessible for $\xi \geq 0.5$. Double Higgs production in the channel $pp \to hhjj$ is considerably more challenging to detect due to the hadronic final states which will be covered by the large QCD background.

A similar analysis for CLIC was performed in [15]. We find that although vector boson scattering is relevant at CLIC, double Higgs production yields a far better sensitivity on ξ. Considering only double Higgs production, CLIC can probe a compositeness scale of $4\pi f \sim 30$ TeV with $\sqrt{s} = 3$ TeV and an integrated luminosity of 1 ab^{-1}. As will be described in more detail in Section 2, we find that CLIC could have an excellent sensitivity on the parameters a, b and d_3 and is sensitive to ξ as low as $\xi \sim 0.005$, i.e. $4\pi f \sim 43$ TeV, for $\sqrt{s} = 5$ TeV. The potential reach of CLIC and the upgraded LHC as well as recent bounds on the parameters space are summarized in Figure 1. Bounds come from current experimental constraints in direct resonance searches in the $WZ \to 3l$ final state at CMS with 4.7 fb^{-1} integrated luminosity at 7 TeV [16, 17]. Further limits are set by electroweak precision tests. The results are presented as the reach in the $\xi - m_\rho$ plane. As can be seen, CLIC is sensitive to the full parameter space.

In Section 3, triple Higgs production is studied. Although the SM cross section is of the order of magnitude of a few ab and therefore too small to be detected at CLIC, this process provides valuable insight into the underlying structure of the model. We show that a process involving an odd number of NG bosons is forbidden in a symmetric coset as in $SO(5)/SO(4)$ which implies that the scattering of $V_LV_L \to hhh$ is not growing with the energy despite naive expectations. A model with an asymmetric coset space or a non-σ-model, however, does not show this cancellation. The cross section of the same process will be two or three orders of magnitude larger and detectable at CLIC.

In conclusion, we find that a multi-TeV electron-positron collider will allow us to make precision measurements on a Higgs-like scalar, precise enough to distinguish between various scenarios and to gain more insight into the underlying structure of the model. It is therefore a perfect machine to probe the strong and composite nature of the Higgs.

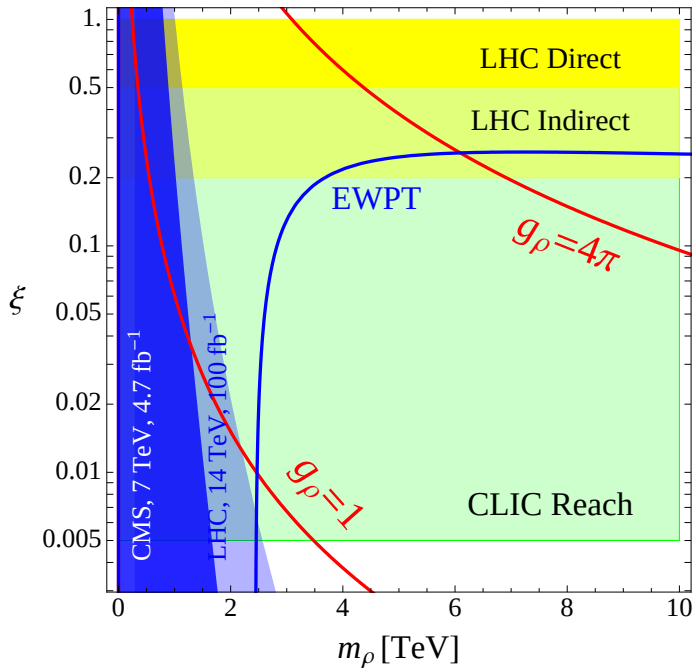

Figure 1: Summary plot of the current constraints and prospects for direct and indirect probes of the strong interactions triggering electroweak symmetry breaking. m_ρ is the mass of the vector resonances and $\xi = (v/f)^2$. The dark yellow band denotes the LHC sensitivity on ξ from WW scattering and strong double Higgs production measurements, while in the light yellow band, ξ can be measured via single Higgs processes. The green band corresponds to the CLIC sensitivity on ξ. The dark and light blue regions on the left are the current limit on resonance mass and coupling from the direct search at the LHC in $WZ \to 3l$ final state with 4.7 fb^{-1} integrated luminosity at 7 TeV [16, 17] and its proper rescaling for LHC at 14 TeV with 100 fb^{-1}. Finally, electroweak precision data favors the region below the blue thick line (the Higgs mass is assumed to be 120 GeV and the vector resonance contribution to ε_3 is taken to be $\Delta\varepsilon_3 = 4m_W^2/(3m_\rho^2)$). The domain of validity of our predictions depends on the strong coupling g_ρ, $1 < g_\rho < 4\pi$, and is between the two red lines. This figure is updated from Ref. [15].

2. Double Higgs Production

Double Higgs production was studied to extract the sensitivity on the couplings b and d_3. The scattering amplitude $V_L V_L \to hh$ depends on these parameters and can thus be written as:

$$\mathscr{A} = a^2 \left(\mathscr{A}_{SM} + \mathscr{A}_1 \delta_b + \mathscr{A}_2 \delta_{d_3}\right), \tag{2.1}$$

where $\mathscr{A}_{SM}$ is the SM amplitude and:

$$\delta_b \equiv 1 - \frac{b}{a^2}, \qquad \delta_{d_3} \equiv 1 - \frac{d_3}{a}. \tag{2.2}$$

The part of the amplitude growing with the energy at large energies will be $\mathscr{A}_1$, while $\mathscr{A}_2$ describes the behavior at threshold. We studied the parameters δ_b and δ_{d_3} in the process $e^+e^- \to \nu\bar{\nu}hh$ assuming a negligible background and full signal reconstruction. In order to disentangle the two parameters we used two kinematical cuts, one on the invariant mass of the two Higgses and the

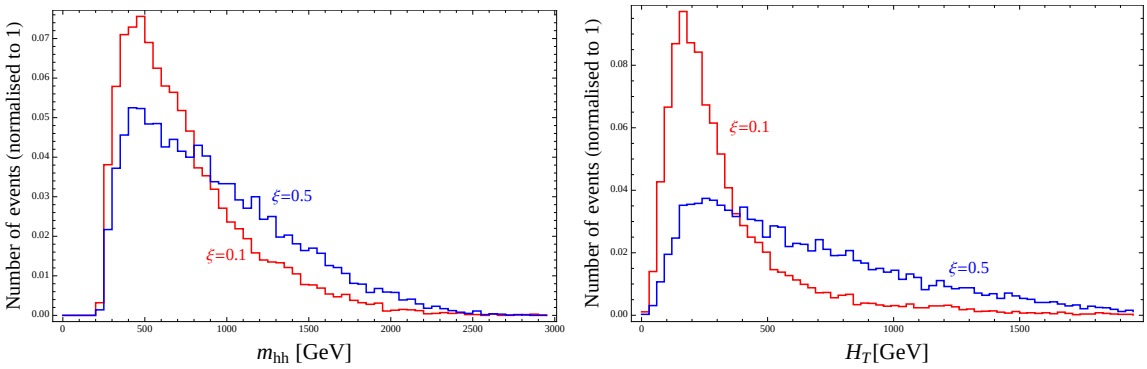

Figure 2: m_{hh} and H_T distributions for $e^+e^- \to hh\nu\bar{\nu}$ for $\sqrt{s} = 3\,\text{TeV}$ and $m_h = 120\,\text{GeV}$. The plots have been obtained without any cuts imposed.

other on the scalar sum of the transverse momenta: $m_{hh} \leq m_{hh}^-$ and $H_T \geq H_T^+$. The distributions corresponding to these two kinematic variables are shown in Figure 2. The optimal cut values were determined by requiring them to maximize the determinant of the matrix of second derivatives of the χ^2-fit. The error on either of the parameters δ_b, δ_{d_3} is then obtained by marginalizing the χ^2 with respect to the other parameter. For more details on the analysis see Refs. [15] and [8]. The sensitivities expected at CLIC at $\sqrt{s} = 3$ TeV are shown in Table 1. As can be seen, CLIC is sensitive to the entire parameter space.

For comparison, we also show the corresponding sensitivities for the ILC in Table 2. The dominant process at energies around the threshold $\sqrt{s} \sim M_Z + 2m_H$ is double Higgsstrahlung [7]. Weak boson fusion processes only take over at higher energies due to their growth with energy. We thus considered the process $e^+e^- \to Zhh$ and made only one cut on the invariant mass of the Higgs pair. We find that the ILC is only sensitive to large values of δ_b and does not cover the full parameter space.

δ_b	δ_{d_3}						
	-0.5	-0.3	-0.1	0	0.1	0.3	0.5
0	(0.02, 0.2)	(0.02, 0.1)	(0.01, 0.08)	(0.01, 0.06)	(0.01, 0.06)	(0.01, 0.05)	(0.01, 0.05)
0.01	(0.02, 0.2)	(0.01, 0.1)	(0.01, 0.07)	(0.01, 0.06)	(0.01, 0.06)	(0.01, 0.05)	(0.009, 0.05)
0.02	(0.02, 0.2)	(0.01, 0.1)	(0.01, 0.07)	(0.009, 0.06)	(0.009, 0.06)	(0.009, 0.5)	(0.009, 0.05)
0.03	(0.01, 0.2)	(0.01, 0.1)	(0.01, 0.07)	(0.009, 0.06)	(0.009, 0.05)	(0.008, 0.05)	(0.008, 0.05)
0.05	(0.01, 0.1)	(0.01, 0.09)	(0.008, 0.06)	(0.008, 0.06)	(0.008, 0.05)	(0.008, 0.05)	(0.008, 0.04)
0.1	(0.009, 0.1)	(0.008, 0.07)	(0.007, 0.06)	(0.007, 0.05)	(0.007, 0.05)	(0.007, 0.04)	(0.007, 0.04)
0.2	(0.008, 0.08)	(0.007, 0.06)	(0.007, 0.05)	(0.007, 0.05)	(0.007, 0.04)	(0.007, 0.04)	(0.007, 0.04)
0.3	(0.007, 0.06)	(0.007, 0.05)	(0.007, 0.05)	(0.007, 0.05)	(0.007, 0.04)	(0.007, 0.04)	(0.007, 0.04)
0.4	(0.007, 0.05)	(0.007, 0.05)	(0.007, 0.05)	(0.007, 0.05)	(0.006, 0.04)	(0.006, 0.04)	(0.007, 0.04)
0.5	(0.007, 0.05)	(0.007, 0.05)	(0.006, 0.04)	(0.006, 0.04)	(0.006, 0.04)	(0.006, 0.04)	(0.006, 0.04)

Table 1: Statistical errors $(\Delta\delta_b, \Delta\delta_{d3})$ on the parameters δ_b and δ_{d_3} for $\sqrt{s} = 3\,\text{TeV}$, $L = 1\,\text{ab}^{-1}/a^4$ and $m_h = 120\,\text{GeV}$. The value of the optimized cuts ranges in the interval $H_T^+ = 250 - 450\,\text{GeV}$, $m_{hh}^- = 450 - 650\,\text{GeV}$.

δ_b	δ_{d_3}						
	-0.5	-0.3	-0.1	0	0.1	0.3	0.5
0	(0.27,0.47)	(0.27,0.47)	(0.27,0.48)	(0.27,0.48)	(0.27,0.48)	(0.28,0.49)	(0.26,0.47)
0.01	(0.26,0.47)	(0.27,0.48)	(0.27,0.48)	(0.27,0.48)	(0.27,0.49)	(0.28,0.49)	(0.26,0.48)
0.03	(0.26,0.47)	(0.27,0.48)	(0.27,0.48)	(0.27,0.48)	(0.27,0.49)	(0.28,0.49)	(0.27,0.48)
0.05	(0.26,0.47)	(0.27,0.48)	(0.27,0.48)	(0.27,0.48)	(0.28,0.49)	(0.28,0.50)	(0.26,0.47)
0.1	(0.26,0.46)	(0.27,0.47)	(0.27,0.48)	(0.27,0.49)	(0.28,0.49)	(0.27,0.49)	(0.27,0.49)
0.2	(0.26,0.46)	(0.26,0.47)	(0.27,0.48)	(0.28,0.49)	(0.28,0.49)	(0.28,0.51)	(0.28,0.51)
0.3	(0.26,0.45)	(0.28,0.46)	(0.27,0.48)	(0.27,0.48)	(0.28,0.50)	(0.29,0.52)	(0.29,0.53)
0.4	(0.25,0.45)	(0.26,0.45)	(0.27,0.47)	(0.27,0.48)	(0.28,0.49)	(0.28,0.51)	(0.29,0.53)
0.5	(0.25,0.45)	(0.26,0.45)	(0.26,0.47)	(0.26,0.47)	(0.27,0.49)	(0.28,0.50)	(0.28,0.52)

Table 2: Statistical errors $(\Delta\delta_b, \Delta\delta_{d3})$ on the parameters δ_b and δ_{d_3} for $\sqrt{s} = 500\,\text{TeV}$, $L = 1\,\text{ab}^{-1}/a^4$ and $m_h = 120\,\text{GeV}$. The value of the optimized cut ranges in the interval $m_{hh}^+ = 270 - 315\,\text{GeV}$.

3. Triple Higgs Production

At CLIC, a triple Higgs final state can be produced by the process $e^+e^- \to \nu\bar{\nu}W^+W^- \to \nu\bar{\nu}hhh$. Naively we would expect the scattering cross section of two longitudinal vector bosons into three Higgs bosons, $\sigma(V_LV_L \to hhh)$, to grow with the energy as s^2. However, a closer look at the symmetry structure of the $SO(5)/SO(4)$ coset reveals a cancellation which is a distinct feature of a symmetric coset space. In this case there is the discrete internal automorphism P_π:

$$\begin{aligned} T^a &\to +T^a, \\ T^{\hat{a}} &\to -T^{\hat{a}}, \end{aligned} \tag{3.1}$$

where T^a and $T^{\hat{a}}$ are the unbroken and broken $SO(5)$ generators respectively. This implies that the NG bosons are odd: $\pi^{\hat{a}} \to -\pi^{\hat{a}}$. Consequently, any process with an odd number of NG bosons is forbidden by this symmetry. P_π is only weakly broken by the gauge couplings which is why the process is not strictly zero but suppressed. The expected energy behavior of the amplitude for the partonic processes is summarised in Table 3.

Polarisation	Amplitude for	
	symmetric coset	asymmetric coset
$LL \to hhh$	g^2v/f^2	E^2v/f^4
$LT \to hhh$	Eg/f^2	
$TT \to hhh$	g^2v/f^2	

Table 3: Energy growth of partonic amplitudes in a symmetric and asymmetric coset.

We have confirmed this cancellation by an explicit computation in the gaugeless limit $g = g\prime = 0$. From the Lagrangian in Eqn. (1.1), we find three distinct diagrams, depicted in Fig. 3, and their crossings contributing to the process $\pi\pi \to hhh$. Individually each of them is growing with the energy. Summing and considering all the crossings carefully leads to an expression for the amplitude depending explicitly on the parameters a, b and b_3:

$$\mathscr{A}(\pi\pi \to hhh) = \frac{is}{v^3}\left(4ab - 4a^3 - 3b_3\right). \tag{3.2}$$

Substituting the values given in Eq. (1.3) shows that the energy growing part of the amplitude vanishes as expected for a symmetric coset.

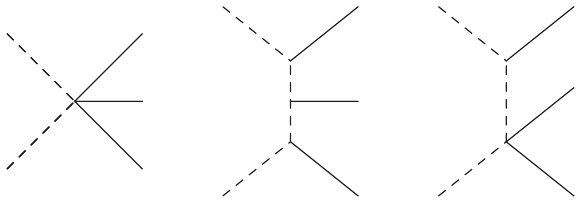

Figure 3: The leading diagrams contributing to the $V_L V_L \to hhh$ amplitude. The dashed line represents the NG bosons π, while the solid line depicts the Higgs h. The sum of these diagrams with all their crossings cancels exactly in the gaugeless limit.

The dominant contribution to the cross section in a symmetric coset comes thus from the process $V_L V_T \to hhh$ instead. The cross section is expected to grow as s. To obtain an estimate, we computed this contribution analytically using an effective description for the strongly interacting light Higgs (SILH) with the following Lagrangian [5]:

$$\mathscr{L}_{\text{SILH}} = \mathscr{L}_{\text{SM}} + \frac{c_H}{2f^2}\partial^\mu\left(H^\dagger H\right)\partial^\mu\left(H^\dagger H\right). \tag{3.3}$$

This parameterization is related to the σ-model Lagrangian in Eq. (1.1) by the following field redefinition:

$$h \to h - \frac{c_H \xi}{2}\left(h + \frac{h^2}{v} + \frac{h^3}{3v^2}\right). \tag{3.4}$$

The dependence of the parameters a, b and b_3 on c_H is thus given by:

$$a = 1 - \frac{c_H}{2}\xi, \qquad b = 1 - 2c_H\xi, \qquad b_3 = -\frac{4}{3}c_H\xi. \tag{3.5}$$

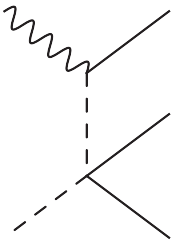

Figure 4: The dominant diagram contributing to the $V_L V_T \to hhh$ cross-section in the forward region. The dashed line represents the NG bosons π, the solid line depicts the Higgs h and the wavy line the transverse components of W. All three crossings of this diagram have to be taken into account

Since we expect a singularity in the forward region, at high energies the total cross section for $V_L V_T \to hhh$ will be dominated by this contribution and it is sufficient to consider the collinear limit.

This simplifies the computation considerably since only 3 diagrams, shown in Fig. 4, have to be taken into account. We neglect diagrams suppressed by c_H^2 and subleading in energy. Considering only a single diagram consisting of a $W\pi h$ and a $\pi\pi hh$ vertex for the process $W_T(p_1)+\pi(p_2)\to h(p_3)+h(p_4)+h(p_5)$ leads to the matrix element:

$$\mathscr{M}^\mu = -\frac{c_H g}{2f^2}\frac{(p_1^\mu - 2p_3^\mu)(p_4+p_5)^2}{(p_1-p_3)^2-m_W^2}. \tag{3.6}$$

Working in the high energy limit, where $m_h, m_W \ll E$ and taking crossings and symmetry factor into account we can integrate over the 3-body phase space and find the following leading term in the cross section:

$$\sigma(W_L W_T \to hhh) = \frac{c_H^2 g^2}{12288\pi^3 f^4} s \log\frac{s}{m_W^2} + \mathscr{O}(s), \tag{3.7}$$

which shows the expected energy growth proportional to s. The logarithmic enhancement originates from a pole in the θ-integral which diverges for small values of θ, i.e. in the forward region. This estimate agrees with a simulation in MadGraph 5 [18].

The behaviour of the partonic cross section with the energy and ξ in a symmetric coset are depicted in Figure 5. The scattering of two longitudinal components is constant while $V_L V_T \to hhh$ grows with the energy as s and at some point wins over the first. The transverse components are constant. In general, cross-sections are larger for bigger values of ξ.

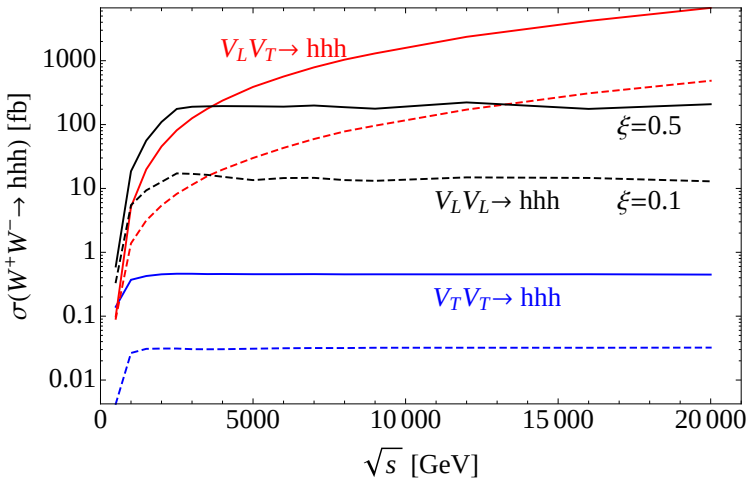

Figure 5: Partonic cross-section vs energy for $V_L V_L \to hhh$, $V_L V_T \to hhh$ and $V_T V_T \to hhh$ for $\xi = 0.1$ and $\xi = 0.5$ in a symmetric coset. Only $V_L V_T \to hhh$ grows with the energy, while the contribution from $V_L V_L \to hhh$ is constant due to the cancellation.

This cancellation is a distinct feature of a symmetric coset space and would not be present in an asymmetric coset space or a non-σ-model. This property enables us to distinguish between the two scenarios. The cross section in the σ-model with a symmetric coset is of the order of magnitude of a few ab, while it goes up to a few hundred ab in the asymmetric coset, depending on the choice of parameters. The former will be very challenging if not impossible to detect at CLIC. However, a cross section of a few hundred ab is sizable enough to be seen. Some typical values for symmetric

and asymmetric coset spaces are shown in Table 4. If a Higgs boson will be found at the LHC, the presence or lack of this process at CLIC would therefore shed light on the underlying structure of the symmetry pattern of the model.

	coset	ξ						
		0	0.01	0.05	0.1	0.5	0.7	0.99
cross section [ab]	✓	0.36	0.38	0.50	0.76	4.20	4.65	0.30
	X	2064						

Table 4: Cross section for the process $e^+e^- \to \nu\bar{\nu}hhh$ for $\sqrt{s} = 3$ TeV. The upper line shows cross sections for a symmetric coset for various values of ξ. Below is the cross section for an asymmetric coset which is indeed a few orders of magnitude larger which demonstrates the cancellation in a symmetric coset.

Acknowledgments

This work has been done in collaboration with Roberto Contino, Christophe Grojean, Duccio Pappadopulo and Riccardo Rattazzi. I would like to thank the organizers of the Corfu Summer Institute 2011 for an interesting and lively school on such a fantastic island. This research project has been supported by a Marie Curie Early Initial Training Network Fellowship of the European Community's Seventh Framework Programme under contract number (PITN-GA-2008-237920-UNILHC).

References

[1] **ATLAS** Collaboration, G. Aad et. al., *Combined search for the Standard Model Higgs boson using up to* 4.9 fb^{-1} *of pp collision data at sqrt*$(s) = 7$ *TeV with the ATLAS detector at the LHC*, (2012), [hep-ex/2012.02.044]

[2] **CMS** Collaboration, S. Chatrchyan et. al., *Combined results of searches for the standard model Higgs boson in pp collisions at sqrt*$(s) = 7$ *TeV*, (2012), [hep-ex/1202.14888]

[3] The **TEVNPH** Working Group for the **CDF** Collaboration and **D0** Collaboration, *Combined CDF and D0 Search for Standard Model Higgs Boson Production with up to 10.0* fb^{-1} *of Data*, (2012), [hep-ex/1203.37748]

[4] P. Giardino, K. Kannike, M. Raidal, A. Strumia, *Reconstructing Higgs boson properties from the LHC and Tevatron data*, (2012), [hep-ph/1203.42548]

[5] G. Giudice, C. Grojean, A. Pomarol, R. Rattazzi, *The Strongly-Interacting Light Higgs*, *JHEP* **06** (2007) 045, [hep-ph/0703164]

[6] R. Contino, C. Grojean, M. Moretti, F. Piccinini, R. Rattazzi, *Strong Double Higgs Production at the LHC*, *JHEP* **1005** (2010) 089, [hep-ph/1002.1011]

[7] V. Barger, T. Han, P. Langacker, B. McElrath, P. Zerwas, *Effects of genuine dimension-six Higgs operators*, *Phys.Rev.* **D 67** (2003) 115001, [hep-ph/0301097]

[8] A. Ioannisian et. al., *Physics and Detectors at CLIC: CLIC Conceptual Design Report*, CERN-2012-003, [ins-det/1202.5940]

[9] J. Brau, Y. Okada, W. Nicholas et. al., *ILC Reference Design Report Volume 1 - Executive Summary*, [acc-ph/0712.1950]

[10] K. Agashe, R. Contino, A. Pomarol, *The Minimal Composite Higgs Model*, *Nucl. Phys.* **B 719** (2005) 165, [hep-ph/0412089]

[11] R. Contino, L. Da Rold, A. Pomarol *Light custodians in natural composite Higgs models*, *Phys. Rev.* **D 75** (2007) 055014, [hep-ph/0612048]

[12] R. Contino, D. Marzocca, D. Pappadopulo, R. Rattazzi, *On the effect of resonances in composite Higgs phenomenology*, *JHEP* **1110** (2011) 081, [hep-ph/1109.1570]

[13] R. Barbieri, B. Bellazzini, V. Rychkov, A. Varagnolo, *The Higgs boson from an extended symmetry*, *Phys.Rev.* **D 76** (2007) 115008, [hep-ph/0706.0432]

[14] R. Contino, *The Higgs as a Composite Nambu-Goldstone Boson*, *TASI Lectures* (2010), [hep-ph/1005.4269]

[15] R. Contino, C. Grojean, D. Pappadopulo, R. Rattazzi, A. Thamm *in preparation*

[16] **CMS** Collaboration, S. Chatrchyan et.al., *CMS Physics Analysis Summary. Searches for W' (or techni-rho) to WZ*, CMS (2011), 1-14. [CMS Public Results]

[17] **CMS** Collaboration, S. Chatrchyan et.al., *Search for exotic particles decaying to the WZ final state with the CMS Experiment*, (2012), [CMS Public Results]

[18] J. Alwall, M. Herquet, F. Maltoni, O. Mattelaer, T. Stelzer", *MadGraph 5 : Going Beyond*, *JHEP* **1106** (2011) 128, [hep-ph/1106.0522]